Mono- and binuclear complexes of rhodium involving a new series of hemilabile *o*-phosphinoaniline ligands†

Lindsay J. Hounjet,[a] Matthias Bierenstiel,‡[a] Michael J. Ferguson,[b] Robert McDonald[b] and Martin Cowie*[a]

Received 10th December 2008, Accepted 16th February 2009
First published as an Advance Article on the web 6th April 2009
DOI: 10.1039/b822170g

Monophosphines of the type Ph_xPAr_{3-x} ($x = 0$, 1 or 2, Ar = *o*-*N*-methylanilinyl) and the diphosphine, $Ar_2PCH_2PAr_2$ (mapm) have been synthesized for use as chelating and/or bridging *P*,*N*-ligands within mono- and binuclear rhodium(I) complexes, respectively. The previously prepared phosphines, $Ph_xPAr'_{3-x}$ ($x = 0$, 1 or 2, Ar′ = *o*-*N*,*N*-dimethylanilinyl) and $Ar'_2PCH_2PAr'_2$ (dmapm), have also been used to prepare analogous mono- and binuclear complexes. Variable temperature ^{1}H NMR spectroscopy of the mononuclear complexes, [RhCl(CO)(L)] (L = $PhPAr_2$, $PhPAr'_2$, PAr_3 and PAr'_3), and line-shape analyses of the resultant spectra indicate the substantially increased lability of the *N*,*N*-dimethylanilinyl donors relative to the related monomethylanilinyl groups. X-Ray structural analyses of the mononuclear complexes suggest that the enhanced Type II hemilability in the dimethylanilinyl complexes compared to their monomethyl analogues results from increased steric interactions involving the coordinated dimethylanilinyl substituents. In the case of the binuclear, dmapm-bridged compound [$Rh_2Cl_2(CO)_2$(μ-dmapm)], there are additional transannular repulsions between the chloro ligand on one metal and the coordinated dimethylanilinyl group on the other, which result in a Rh–Rh separation of over 4.1 Å. For the analogous mapm-bridged species, the transannular interactions between the chloro ligands and the amine hydrogens are in fact attractive, resulting in a much closer Rh–Rh separation (3.450 Å). The chloride substituents of [$Rh_2Cl_2(CO)_2$(μ-mapm)] can be replaced to generate the complexes, [$Rh_2(X)_2(CO)_2$(μ-mapm)] (X = I, CF_3SO_3, CH_3CO_2), the last of which also exhibits pronounced transannular hydrogen-bonding interactions in the solid state.

Introduction

Bi- and multidentate ligands occupy an important position in the chemistry of transition metals.[1–7] Not only do such groups find applications in mononuclear complexes, where they offer additional stability compared to related monodentate ligands, through the chelate effect,[8] they can also be used to bridge two or more metals in multinuclear complexes.[9–18] Multidentate ligands can also be extended to a series of "hybrid" ligands, capable of binding to the metal(s) through different donor atoms.[19–42] This not only introduces the flexibility of ligand fine-tuning, in which the metal(s) can be sterically and electronically "tuned" through the use of different combinations of donor sites within these hybrids, but also introduces the concept of hemilability,[19–38] in which one or more donor sites in the multidentate ligand bind more strongly to the metal(s) under study while other donor site(s) bind weakly. These labile donors are capable of stabilizing the complex in the absence of substrate, while being readily and reversibly displaced by the appropriate substrate. The resulting "incipient coordinative unsaturation" has obvious applications in catalysis,[20–27,35] in which the labile donor stabilizes the catalyst precursor prior to substrate coordination and assists in displacing the catalyst-modified substrate, regenerating the catalyst precursor, after the transformation is complete. In this context, ligands containing "soft" phosphorus and "hard" nitrogen donors have found many applications as hemilabile ligands in the chemistry of low-valent, late-transition-metal complexes,[20–24,26–38] in which phosphorus binds strongly while nitrogen is more labile.

We have sought to combine two of the above themes through the use of diphosphine ligands with pendent amine groups, in which the diphosphine moiety binds effectively to and bridges a pair of late metals, holding them in close proximity, while the chelating amines function as labile groups. In earlier studies we[43] and others[44–48] used bis(di(*o*-*N*,*N*-dimethylanilinyl) phosphino)methane (dmapm = $Ar'_2PCH_2PAr'_2$; Ar′ = *o*-C_6H_4-NMe_2) as a bridging diphosphine ligand that has chelating, hemilabile dimethylanilinyl groups. However, in our study we proposed that unfavorable steric repulsions involving the pairs of methyl substituents on the anilinyl groups have appeared to inhibit close approach of the adjacent metals, so we subsequently set out to synthesize the somewhat less bulky monomethylanilinyl analogue, $Ar_2PCH_2PAr_2$ (mapm; Ar = *o*-C_6H_4NHMe), in order to reduce the steric demand of the amine donors. In addition, we set out to prepare a series of monophosphine analogues of mapm in order to compare the reactivities of related mononuclear and binuclear diphosphine-bridged species, thereby gaining information on possible influences of adjacent metals on substrate activation

[a]*Department of Chemistry, University of Alberta, Edmonton, Alberta, Canada T6G 2G2. E-mail: martin.cowie@ualberta.ca; Fax: +1 (1)780 4928231; Tel: +1 (1)780 4925581*
[b]*X-Ray Crystallography Laboratory, University of Alberta, Edmonton, Alberta, Canada T6G 2G2*
† CCDC reference numbers 713707–713713. For crystallographic data in CIF or other electronic format see DOI: 10.1039/b822170g
‡ Present address: Department of Chemistry, Cape Breton University, Sydney, Nova Scotia, Canada, B1P 6L2

and on the possibility of cooperative substrate activation by the adjacent metals. Such cooperative substrate activation has been elegantly demonstrated in a related dirhodium system[16] that utilized a non-labile tetraphosphine ligand in which the central pair of phosphorus nuclei bridged the metals while the outer pair each chelated to a different metal.

A further aspect of interest in these monomethylanilinyl phosphines is the possibility of deprotonating the amine groups yielding amido functionalities. The reversible transformation of chelating amine to amido groups has generated enormous recent interest in the catalytic hydrogenation of polar substrates such as ketones.[49–51]

In this paper we report the synthesis of a series of hybrid monomethylanilinyl phosphine ligands and the generation of a series of mononuclear and binuclear complexes of rhodium using these hybrid ligands. The steric influences of these monomethylanilinyl derivatives with regards to their lability and their structural influences are compared with the analogous species containing the dimethylanilinyl groups.

Experimental

General comments

All solvents were deoxygenated, dried (using appropriate drying reagents) and distilled before use and stored under nitrogen. Reactions were performed under an argon atmosphere using standard Schlenk techniques. $RhCl_3{\cdot}3H_2O$, Ph_2PCl, $PhPCl_2$, PCl_3 and $Cl_2PCH_2PCl_2$ were purchased from Strem Chemicals. *n*-BuLi and *t*-BuLi were purchased from Sigma-Aldrich. Dry CO_2(g) was purchased from Supelco. The compounds $[Rh(\mu\text{-}Cl)(COD)]_2$[52] (COD = 1,5-cyclooctadiene) and $[Rh(\mu\text{-}Cl)(CO)_2]_2$[53] were prepared by the literature routes. The monophosphine ligands, bis(*o*-*N*,*N*-dimethylanilinyl)-phenylphosphine ($PhPAr'_2$), tris(*o*-*N*,*N*-dimethylanilinyl)phosphine (PAr'_3),[54] and the diphosphine ligand, bis(di(*o*-*N*,*N*-dimethylanilinyl)phosphino)methane (dmapm),[44] were prepared as previously reported. *o*-Bromo-*N*,*N*-dimethylaniline was prepared from commercially available *o*-bromoaniline by exhaustive methylation with dimethylsulfate.[55] NMR spectra were recorded on Bruker AM-400, Varian Inova-400 or Varian Unity-500 spectrometers operating at 400.0, 399.8 or 499.8 MHz, respectively, for ^{1}H; at 161.9, 161.8 or 202.3 MHz, respectively, for ^{31}P; and at 100.6, 100.6 or 125.7 MHz, respectively, for ^{13}C nuclei. *J* values are given in Hz and overlapping, unresolved aromatic ^{13}C NMR signals, observed in the typical 80–120 ppm range, are not reported. Spectroscopic data for all metal complexes (**5–14**) are provided in Table 1. Solution-phase infrared spectra (KBr cell) were recorded on either a FT-IR Bomem MB-100 spectrometer or a Nicolet Avatar 370 DTGS spectrometer. Elemental analyses were performed by the Microanalytical Laboratory of the University of Alberta. Electrospray ionization mass spectra were run on a Micromass Zabspec spectrometer in the departmental MS facility. In all cases, the distribution of isotope peaks for the appropriate parent ion matched very closely that calculated from the formulation given. SpinWorks version 2.5.5[56] was used for line-shape analyses and NMR spectral simulations. Conductivity measurements were carried out under inert conditions on 10^{-3} M solutions of $[Rh_2(OTf)_2(CO)_2(\mu\text{-mapm})]$ (**12**) and $[Rh_2(OAc)_2(CO)_2(\mu\text{-mapm})]$ (**14**) in dry nitromethane using a Yellow Springs Instrument Model 31 conductivity bridge. For these species the molar conductivities were determined as Λ = 23 and 12 cm^2 Ω^{-1} mol^{-1}, respectively.

Preparation of *P*,*N*-ligands

(a) Diphenyl(*o*-*N*-methylanilinyl)phosphine (Ph_2PAr) 1. In a 200 mL Schlenk flask *N*-methylaniline (1.73 mL, 15.9 mmol) was dissolved in 30 mL of freshly distilled, dry tetrahydrofuran (THF) and cooled to −78 °C (acetone/dry-ice bath). *n*-BuLi (2.5 M in hexanes, 6.3 mL, 16 mmol) was added dropwise *via* syringe resulting in immediate slow gas evolution and formation of a white precipitate. The reaction mixture was allowed to warm to ambient temperature (approx. 45 min) after which CO_2(g) was passed through the reaction mixture *via* a syringe needle attachment at a moderate rate (approx. 0.5 mL s^{-1}) for 15 min resulting in a clear, light yellow solution. The solution was allowed to stir for 15 min before cooling to −78 °C. *t*-BuLi (1.7 M in THF, 11 mL, 19 mmol) was added dropwise *via* syringe producing a white precipitate in a bright yellow-orange solution. The reaction mixture was stirred at −78 °C for 5 min, allowed to warm to −35 °C (acetonitrile/dry-ice bath) and stirred for 1 h to generate the dilithiated intermediate. Chlorodiphenylphosphine (2.85 mL, 15.9 mmol) in 15 mL of dry THF was added dropwise *via* syringe. The cooling bath was removed and the reaction mixture was allowed to warm to ambient temperature. HCl (2 M, 15 mL) was added carefully to quench the reaction, leading to release of CO_2(g). After cessation of CO_2(g) effervescence, the solution was neutralized with a 30% (w/w) KOH–H_2O solution. 50 mL of water was then added and the aqueous layer was extracted with 3 × 50 mL of Et_2O. The combined organic layers were then washed with 100 mL of water, dried over anhydrous Na_2SO_4, filtered and the solvent was removed *in vacuo*. The *o*-phosphinoaniline was recrystallized from approx. 50 mL of boiling ethanol (2.78 g, 60.1%) yielding a white, crystalline product (found: C, 78.11; H, 6.30; N, 4.81. Calc. for $C_{19}H_{18}NP$: C, 78.33; H, 6.23; N, 4.81%); δ_H(400 MHz; CD_2Cl_2; Me_4Si) 2.84 (3H, s/br, CH_3), 4.86 (1H, m/br, NH), 6.65 (2H, m, H_{Ar}), 6.79 (1H, m, H_{Ar}), 7.33 (11H, m, H_{Ar}). δ_C(101 MHz; CD_2Cl_2; Me_4Si) 30.8 (1C, s, CH_3). δ_P(162 MHz; CD_2Cl_2; H_3PO_4) −21.8 (s). HRMS (EI, 70 eV). Found: *m*/*z* 291.11697 for [M]$^+$. Calc. for $C_{19}H_{18}NP$: *m*/*z* 291.11768.

(b) Di(*o*-*N*-methylanilinyl)phenylphosphine ($PhPAr_2$) 2. The dilithiated intermediate was prepared from *N*-methylaniline (2.10 mL, 19.3 mmol) as described in part (a). Dichlorophenylphosphine (1.31 mL, 9.65 mmol) was added dropwise *via* syringe and the mixture was allowed to warm slowly to ambient temperature. The resulting solution was then acidified, neutralized, extracted, dried and filtered as described in part (a). The solvent was removed *in vacuo* and the *o*-phosphinoaniline was cleanly precipitated from approx. 50 mL of boiling ethanol (1.40 g, 45.4%) yielding a white powder (found: C, 74.64; H, 6.49; N, 8.66. Calc. for $C_{20}H_{21}N_2P$: C, 74.98; H, 6.61; N, 8.74%); δ_H(400 MHz; CD_2Cl_2; Me_4Si) 2.85 (6H, s/br, CH_3), 4.71 (2H, m/br, NH), 6.67 (4H, m, H_{Ar}), 6.82 (2H, m, H_{Ar}), 7.37 (7H, m, H_{Ar}). δ_C(101 MHz; CD_2Cl_2; Me_4Si) 30.9 (2C, s, CH_3). δ_P(162 MHz; CD_2Cl_2; H_3PO_4) −38.0 (s). HRMS (EI, 70 eV). Found: *m*/*z* 320.14380 for [M]$^+$. Calc. for $C_{20}H_{21}N_2P$: *m*/*z* 320.14423.

(c) Tri(*o*-*N*-methylanilinyl)phosphine (PAr_3) 3. The dilithiated intermediate was prepared from *N*-methylaniline (2.10 mL,

Table 1 Spectroscopic data for the rhodium complexes

Compound	IR/cm^{-1} [a]	NMR [b] $\delta(^{31}P\{^1H\})$/ppm [c]	$\delta(^1H)$/ppm [d]	$\delta(^{13}C\{^1H\})$/ppm [d]
[RhCl(CO)(Ph$_2$PAr)] (**5**)	1992 (s)	58.0 (d, $^1J_{RhP}$ = 169 Hz, 1P)[k]	NH: 5.57 (br, 1H)[k] NMe: 2.87 (d, $^3J_{HH}$ = 6.5 Hz, 3H)[k]	CO: 189.3 (dd, $^1J_{RhC}$ = 73 Hz, $^2J_{PC}$ = 18 Hz)[k] NMe: 44.1 (s)[k]
[RhCl(CO)(PhPAr$_2$)] (**6**)	1996 (s)	41.7 (d, $^1J_{RhP}$ = 156 Hz, 1P)[k]	NH: 5.73 (br, 2H)[k] NMe: 2.73 (br, 6H)[k]	CO: 188.9 (dd/br, $^1J_{RhC}$ = 55 Hz)[k] NMe: 43.9 (s/br, 1C), 30.2 (s/br)[k]
			NH: 7.20 (3H),[l] 6.37 (br, 1H), 6.32 (br, 1H), 5.95 (br, 3H)[g] NMe: 2.88 (d, $^3J_{HH}$ = 5.9 Hz, 3H), 2.77 (d, $^3J_{HH}$ = 5.0 Hz, 3H), 2.62 (d, $^3J_{HH}$ = 5.7 Hz, 9H), 2.56 (d, $^3J_{HH}$ = 4.8 Hz, 9H)[g]	
[RhCl(CO)(PAr$_3$)] (**7**)	1994 (s)	27.9 (d, $^1J_{RhP}$ = 149 Hz, 1P)[k]	NH: 7.00 (1H),[l] 5.04 (br, 1H), 4.64 (br, 1H)[k] NMe: 2.79 (br, 9H)[k]	CO: 189.6 (dd, $^1J_{RhC}$ = 73 Hz, $^2J_{PC}$ = 16 Hz)[k] NMe: 30.3 (s/br)[k]
			NH: 7.38 (1H),[l] 5.23 (br, 1H), 4.36 (br, 1H)[i] NMe: 2.81 (d, $^3J_{HH}$ = 5.0 Hz, 3H), 2.71 (d, $^3J_{HH}$ = 4.9 Hz, 3H), 2.63 (d, $^3J_{HH}$ = 6.0 Hz, 3H)[i]	
[RhCl(CO)(PhPAr′$_2$)] (**8**)	1987 (s)	49.7 (d, $^1J_{RhP}$ = 173 Hz, 1P)[k]	NMe$_2$: 2.75 (s, 12H)[k]	CO: 189.1 (dd, $^1J_{RhC}$ = 74 Hz, $^2J_{PC}$ = 17 Hz)[k] NMe$_2$: 48.5 (s)[k]
			NMe$_2$: 3.01 (s/br, 3H), 2.94 (s/br, 3H), 2.69 (s/br, 3H), 1.89 (s/br, 3H)[f]	
[RhCl(CO)(PAr′$_3$)] (**9**)	1988 (s)	37.8 (d, $^1J_{RhP}$ = 186 Hz, 1P)[k]	NMe$_2$: 2.69 (s, 18H)[k]	CO: 190.1 (dd, $^1J_{RhC}$ = 76 Hz, $^2J_{PC}$ = 17 Hz)[k] NMe$_2$: 47.8 (s)[k]
			NMe$_2$: 2.83 (s/br, 9H), 2.34 (s/br, 9H)[f]	
[Rh$_2$Cl$_2$(CO)$_2$(μ-mapm)] (**10**)	2000 (s)	23.3 (m, $^1J_{RhP}$ = 160 Hz, 2P)[e,k]	NH: 7.75 (2H), 6.94 (2H)[k,l] CH$_2$: 3.94 (m, 2H)[k] NMe: 3.17 (d, $^3J_{HH}$ = 6.0 Hz, 6H) 2.78 (d, $^3J_{HH}$ = 4.8 Hz, 6H)[k]	CO: 185.3 (dd, $^1J_{RhC}$ = 71 Hz, $^2J_{PC}$ = 18 Hz)[k] NMe: 42.9 (s, 2C), 30.2 (s, 2C)[k] CH$_2$: 33.7 (t, $^1J_{PC}$ = 31 Hz)[k]
[Rh$_2$Cl$_2$(CO)$_2$(μ-dmapm)] (**11**)	1999 (s)	41.0 (d, $^1J_{RhP}$ = 175 Hz, 2P)[k]	CH$_2$: 4.59 (t/br, $^2J_{PH}$ = 12.4 Hz, 2H)[k] NMe$_2$: 3.70 (s/br, 6H), 2.97 (s/br, 6H), 2.73 (s/br, 6H), 2.53 (s/br, 6H)[k]	CO: 187.6 (dd, $^1J_{RhC}$ = 80 Hz, $^2J_{PC}$ = 28 Hz)[j] NMe$_2$: 52.3 (s, 2C), 51.9 (s, 2C), 47.9 (s, 2C), 47.1 (s, 2C)[j] CH$_2$: 27.3 (t, $^1J_{PC}$ = 29 Hz)[j]
		41.8 (m, $^1J_{RhP}$ = 179 Hz, 2P)[e,h]	CH$_2$: 4.59 (t, $^2J_{PH}$ = 11.6 Hz, 2H)[f] NMe$_2$: 3.68 (s, 6H), 2.86 (s, 6H), 2.70 (s, 6H), 2.27 (s, 6H)[f]	
[Rh$_2$(OTf)$_2$(CO)$_2$(μ-mapm)] (**12**)	2000 (s)	31.5 (m, $^1J_{RhP}$ = 176 Hz, 2P)[e,k]	NH: 7.64 (2H)[k,l], 6.62 (m/br, 2H)[k] CH$_2$: 3.97 (m, 2H)[k] NMe: 3.09 (d, $^3J_{HH}$ = 6.0 Hz, 6H) 2.85 (d, $^3J_{HH}$ = 5.0 Hz, 6H)[k]	N/A (poorly soluble)
[Rh$_2$I$_2$(CO)$_2$(μ-mapm)] (**13**)	2000 (s)	20.3 (m, $^1J_{RhP}$ = 162 Hz, 2P)[e,k]	NH: 7.60 (2H), 6.62 (2H)[k,l] CH$_2$: 3.96 (m, 2H)[k] NMe: 3.25 (d, $^3J_{HH}$ = 6.0 Hz, 6H) 2.76 (d, $^3J_{HH}$ = 5.0 Hz, 6H)[k]	N/A (poorly soluble)
[Rh$_2$(OAc)$_2$(CO)$_2$(μ-mapm)] (**14**)	1991 (s)[m]	28.2 (m, $^1J_{RhP}$ = 155 Hz, 2P)[e,k]	NH: 8.91 (m/br, 2H), 8.12 (m/br, 2H)[k] CH$_2$: 3.81 (m, 2H)[k] NMe: 3.14 (d, $^3J_{HH}$ = 6.0 Hz, 6H), 2.78 (d, $^3J_{HH}$ = 4.8 Hz, 6H)[k]	N/A (slowly decomposes in CD$_2$Cl$_2$)

[a] IR abbreviations: s = strong, m = medium, w = weak. Only ν_{CO} signals given. Dichloromethane solution; in units of cm^{-1}. [b] NMR abbreviations: s = singlet, d = doublet, t = triplet, m = multiplet, br = broad, dd = doublet of doublets. NMR data in CD$_2$Cl$_2$. [c] ^{31}P chemical shifts referenced to external 85% H$_3$PO$_4$. [d] ^{1}H and ^{13}C chemical shifts referenced to tetramethylsilane. Chemical shifts for phenyl groups not given. [e] 2nd-order effects complicate observed signal pattern. [f] NMR data at −80 °C. [g] NMR data at −60 °C. [h] NMR data at −40 °C. [i] NMR data at −20 °C. [j] NMR data at 0 °C. [k] NMR data at 27 °C. [l] Multiplicities of NH signals could not be determined (due to overlap with aromatic proton signals); chemical shifts were determined by gradient correlation spectroscopy (GCOSY) analysis. [m] THF solution.

19.3 mmol) as described in part (a). Trichlorophosphine (0.56 mL, 6.4 mmol) was added dropwise *via* syringe and the mixture was allowed to slowly warm to ambient temperature. The resulting solution was then acidified, neutralized, extracted, dried and filtered as described in part (a). The solvent was removed *in vacuo* and the *o*-phosphinoaniline precipitated from approx. 50 mL of boiling ethanol (0.436 g, 19.4%) yielding an off-white powder; δ_H(400 MHz; CD$_2$Cl$_2$; Me$_4$Si) 2.85 (9H, d/br, $^3J_{HH}$ = 5.0 Hz, CH$_3$), 4.57 (3H, m/br, NH), 6.69 (6H, m, H$_{Ar}$), 6.82 (3H, m, H$_{Ar}$), 7.34 (3H, m, H$_{Ar}$). δ_C(101 MHz; CD$_2$Cl$_2$; Me$_4$Si) 30.8 (3C, s, CH$_3$). δ_P(162 MHz; CD$_2$Cl$_2$; H$_3$PO$_4$) −53.6 (s). HRMS (EI, 70 eV). Found: *m/z* 349.17050 for [M]$^+$. Calc. for C$_{21}$H$_{24}$N$_3$P: *m/z* 349.17078.

(d) Bis(di(*o*-*N*-methylanilinyl)phosphino)methane (mapm) 4. The dilithiated intermediate was prepared from *N*-methylaniline (1.75 mL, 16.2 mmol) as described in part (a). In a 25 mL Schlenk flask bis(dichlorophosphino)methane (0.53 mL, 4.0 mmol) was dissolved in 2 mL of freshly distilled, dry THF. The diphosphine solution was added dropwise over 5 min to the reaction mixture *via* cannula and the mixture was allowed to slowly warm to ambient temperature. The resulting solution was then acidified, neutralized, extracted, dried and filtered as described in part (a). The solvent was removed *in vacuo* and the *o*-phosphinoaniline was cleanly precipitated from approx. 20 mL of boiling ethanol (0.378 g, 18.9%) yielding an off-white powder (found: C, 69.19; H, 6.80; N, 10.76; Calc. for C$_{29}$H$_{34}$N$_4$P$_2$: C, 69.59; H, 6.85; N, 11.19%);

δ_H(400 MHz; CD_2Cl_2; Me_4Si) 2.74 (2H, m, CH_2), 2.77 (12H, d, $^3J_{HH} = 4.8$ Hz, CH_3), 4.62 (4H, m/br, NH), 6.58 (4H, m, H_{Ar}), 6.69 (4H, m, H_{Ar}), 7.24 (8H, m, H_{Ar}). δ_C(100 MHz; CD_2Cl_2; Me_4Si) 21.7 (1C, t, $^1J_{PC} = 16$ Hz, CH_2), 31.1 (4C, s, CH_3). δ_P(162 MHz; CD_2Cl_2; H_3PO_4) −60.9 (s). HRMS (ES^+). Found: m/z 501.23282 for [M^+ + H]. Calc. for $C_{29}H_{35}N_4P_2$: m/z 501.23315.

Preparation of metal complexes

(e) Chlorocarbonyl(diphenyl(*o*-*N*-methylanilinyl)phosphine)rhodium(I) [RhCl(CO)(Ph_2PAr)] 5. In a 50 mL Schlenk flask under anhydrous conditions and Ar atmosphere, [Rh(μ-Cl)(COD)]$_2$ (200 mg, 0.406 mmol) and Ph_2PAr (236 mg, 0.811 mmol) were dissolved in dichloromethane (10 mL) at ambient temperature. CO(g) was passed through the solution for 10 min at an approximate rate of 0.5 mL s^{-1} and the reaction mixture was stirred for 18 h at ambient temperature. The solvent was reduced to approximately 2 mL under vacuum and a yellow solid precipitated upon addition of 20 mL of dry *n*-pentane. The yellow solid was filtered, washed with 10 mL of *n*-pentane and dried *in vacuo* (334 mg, 90.4%). Single crystals suitable for X-ray crystallographic analysis were obtained by dissolving the complex, under Ar atmosphere, in a minimum volume of CH_2Cl_2 and layering the solution with anhydrous *n*-pentane in an NMR tube (found: C, 50.80; H, 3.71; N, 2.96; Cl, 10.63. Calc. for [$C_{20}H_{18}ClNOPRh$]·0.25CH_2Cl_2: C, 50.78; H, 3.89; N, 2.92; Cl, 11.10%).

(f) Chlorocarbonyl(di(*o*-*N*-methylanilinyl)phenylphosphine)rhodium(I) [RhCl(CO)($PhPAr_2$)] 6. The compound was prepared as described in part (e) using [Rh(μ-Cl)(COD)]$_2$ (187 mg, 0.383 mmol) and $PhPAr_2$ (245 mg, 0.765 mmol) and isolated as a yellow solid (305 mg, 81.9%). Single crystals suitable for X-ray crystallographic analysis were obtained by dissolving the complex, under Ar atmosphere, in a minimum volume of CH_2Cl_2 and layering the solution with anhydrous *n*-pentane in an NMR tube (found: C, 48.82; H, 4.08; N, 5.38. Calc. for [$C_{21}H_{21}ClN_2OPRh$]·0.5CH_2Cl_2: C, 48.80; H, 4.19; N, 5.29%).

(g) Chlorocarbonyl(tri(*o*-*N*-methylanilinyl)phosphine)rhodium(I) [RhCl(CO)(PAr_3)] 7.

Method a. The compound was prepared as described in part (e) using [Rh(μ-Cl)(COD)]$_2$ (174 mg, 0.352 mmol) and PAr_3 (246 mg, 0.704 mmol) and isolated as a yellow solid (348 mg, 95.8%). Single crystals suitable for X-ray crystallographic analysis were obtained by dissolving the complex, under Ar atmosphere, in a minimum volume of CH_2Cl_2 and layering the solution with anhydrous *n*-pentane in an NMR tube.

Method b. In a 50 mL Schlenk flask under anhydrous conditions and Ar atmosphere, [Rh(μ-Cl)($CO)_2$]$_2$ (27 mg, 68 μmol) and PAr_3 (48 mg, 0.14 mmol) were dissolved in dry THF (5 mL) at ambient temperature. The yellow solution was stirred for 5 min before 10 mL of dry *n*-pentane were added and the resulting yellow precipitate was allowed to settle before removing the supernatant *via* cannula. The compound was then dried *in vacuo* (61 mg, 86%) producing a yellow solid (found: C, 51.05; H, 4.83; N, 7.83. Calc. for [$C_{22}H_{24}ClN_3OPRh$]: C, 51.23; H, 4.69; N, 8.15%).

(h) Chlorocarbonyl(bis(*o*-*N*,*N*-dimethylanilinyl)phenylphosphine)rhodium(I) [RhCl(CO)($PhPAr'_2$)] 8. The compound was prepared as described in part (e) using [Rh(μ-Cl)(COD)]$_2$ (200 mg, 0.406 mmol) and $PhPAr'_2$ (282 mg, 0.812 mmol) and isolated as a yellow solid (366 mg, 87.5%). Single crystals suitable for X-ray crystallographic analysis were obtained by dissolving the complex, under Ar atmosphere, in a minimum volume of CH_2Cl_2 and layering the solution with anhydrous *n*-pentane in an NMR tube (found: C, 53.49; H, 4.92; N, 5.48. Calc. for [$C_{21}H_{20}ClN_2OPRh$]: C, 53.66; H, 4.89; N, 5.44%).

(i) Chlorocarbonyl(tris(*o*-*N*,*N*-dimethylanilinyl)phosphine)rhodium(I) [RhCl(CO)(PAr'_3)] 9. The compound was prepared as described in part (e) using [Rh(μ-Cl)(COD)]$_2$ (58 mg, 0.13 mmol) and PAr'_3 (92 mg, 0.24 mmol) and isolated as a yellow solid (101 mg, 76.6%). Single crystals suitable for X-ray crystallographic analysis were obtained by dissolving the complex, under Ar atmosphere, in a minimum volume of CH_2Cl_2 and layering the solution with anhydrous *n*-pentane in an NMR tube (found: C, 52.81; H, 5.31; N, 7.32; Cl, 7.43. Calc. for [$C_{25}H_{30}ClN_3OPRh$]·0.11CH_2Cl_2: C, 53.20; H, 5.37; N, 7.41; Cl, 7.57%). Although the crystal structure indicates no dichloromethane content, a microcrystalline sample was analyzed here. Chloride analysis and ^{1}H NMR analysis in $CDCl_3$ (both obtained at approximately the same time) were used to determine dichloromethane content.

(j) Dichlorodicarbonyl(μ-*P*,*N*,*P*′,*N*′-bis(di(*o*-*N*-methylanilinyl)phosphino)methane)dirhodium(I) [$Rh_2Cl_2(CO)_2$(μ-mapm)] 10. In a 50 mL Schlenk flask under anhydrous conditions and Ar atmosphere, [Rh(μ-Cl)($CO)_2$]$_2$ (77 mg, 0.20 mmol) and mapm (103 mg, 0.206 mmol) were dissolved in THF (15 mL) by stirring at ambient temperature. Solvent was slowly removed from the bright red–orange solution by heating to 40 °C under a steady flow of Ar(g). Dichloromethane (3 mL) was added to the resultant orange solids yielding a red solution with a bright-yellow precipitate. The precipitate was isolated by Schlenk filtration, washed three times with 1 mL aliquots of dichloromethane and dried *in vacuo* (118 mg, 71%). Single crystals suitable for X-ray crystallographic analysis were obtained by dissolving the complex, under Ar atmosphere, in a minimum volume of CH_2Cl_2 and layering the solution with anhydrous Et_2O in an NMR tube (found: C, 42.60; H, 3.96; N, 6.15; Cl, 13.67. Calc. for [$C_{31}H_{34}Cl_2N_4O_2P_2Rh_2$]·0.75$CH_2Cl_2$: C, 42.51; H, 3.99; N, 6.25; Cl, 13.68%).

(k) Dichlorodicarbonyl(μ-*P*,*N*,*P*′,*N*′-bis(di(*o*-*N*,*N*-dimethylanilinyl)phosphino)methane)dirhodium(I) [$Rh_2Cl_2(CO)_2$(μ-dmapm)] 11. In a 100 mL Schlenk flask under anhydrous conditions and Ar atmosphere, [Rh(μ-Cl)($CO)_2$]$_2$ (149 mg, 0.383 mmol) and dmapm (227 mg, 0.408 mmol) were dissolved in 10 mL of dichloromethane at ambient temperature and stirred. Stirring was stopped after 30 min and a light Ar(g) stream was left blowing over the saturated red–orange solution for 18 h producing cube-shaped, orange–yellow crystals. The crystals were then washed with 1 mL of dry dichloromethane and dried *in vacuo* (278 mg, 81.5%). Single crystals suitable for X-ray crystallographic analysis were obtained by dissolving the complex, under Ar atmosphere, in a minimum volume of CH_2Cl_2 and layering the solution with anhydrous *n*-pentane in an NMR tube (found: C, 47.35; H, 4.89; N, 6.37. Calc. for [$C_{35}H_{42}Cl_2N_4O_2P_2Rh_2$]: C, 47.27; H, 4.76; N, 6.30%).

(l) Bis (trifluoromethanesulfonato)dicarbonyl(μ - *P*, *N*, *P′*,*N′* - bis(di(*o*-*N*-methylanilinyl)phosphino)methane)dirhodium(I) [Rh_2-$(OTf)_2(CO)_2$(μ-mapm)] 12. In a 25 mL Schlenk tube under anhydrous conditions and Ar atmosphere, [$Rh_2Cl_2(CO)_2$(μ-mapm)] (51 mg, 61 μmol) and AgOTf (34 mg, 13 μmol) were dissolved in 5 mL of dichloromethane at ambient temperature and stirred for 12 h in the dark. The resultant orange–brown slurry was then left unstirred and the precipitate allowed to settle before filtering the orange solution through celite into a 50 mL Schlenk flask. The solvent was removed *in vacuo* and the complex was washed with 1 mL of dichloromethane before drying *in vacuo* (43 mg, 66%) producing an orange solid (found: C, 37.34; H, 3.56; N, 5.63. Calc. for [$C_{33}H_{34}F_6N_4O_8P_2Rh_2S_2$]: C, 37.37; H, 3.23; N, 5.28%).

(m) Diiododicarbonyl(μ-*P*,*N*,*P′*,*N′*-bis(di(*o*-*N*-methylanilinyl)phosphino)methane)dirhodium(I) [$Rh_2I_2(CO)_2$(μ-mapm)] 13. In a 100 mL Schlenk flask under anhydrous conditions and Ar atmosphere, [$Rh_2Cl_2(CO)_2$(μ-mapm)] (106 mg, 0.127 mmol) was dissolved in 10 mL of dichloromethane at ambient temperature and stirred. Under similar conditions, KI (207 mg, 1.25 mmol) was dissolved in 8 mL of methanol at ambient temperature. The KI solution was transferred to the [$Rh_2Cl_2(CO)_2$(μ-mapm)] solution *via* cannula and the resultant orange solution was stirred at ambient temperature for 1 h producing an orange–brown slurry. The solvents were removed *in vacuo* yielding a brown solid. Water (40 mL) was added with stirring and the product was extracted with 3 × 5 mL of dichloromethane into a 50 mL Schlenk flask. The solution was stirred vigorously while adding 15 mL of Et_2O followed by 10 mL of *n*-pentane producing a yellow precipitate which was allowed to settle before the supernatant was decanted. The complex was then dried under a brisk flow of Ar and dried further *in vacuo* (85 mg, 66%) producing a yellow solid (found: C, 36.38; H, 3.43; N, 5.15. Calc. for [$C_{31}H_{34}I_2N_4O_2P_2Rh_2$]: C, 36.64; H, 3.37; N, 5.51%).

(n) Diacetatodicarbonyl(μ-*P*,*N*,*P′*,*N′*-bis(di(*o*-*N*-methylanilinyl)phosphino)methane)dirhodium(I) [$Rh_2(OAc)_2(CO)_2$(μ-mapm)] 14. In a 50 mL Schlenk flask under anhydrous conditions and Ar atmosphere, 25 mL of dry THF was added to [$Rh_2Cl_2(CO)_2$(μ-mapm)] (161 mg, 0.193 mmol) and KOAc (186 mg, 1.90 mmol). The resulting dark-red slurry was stirred for 18 h and then filtered through celite. The solvent volume was reduced to approx. 2 mL *in vacuo* before dry *n*-pentane was added and the resultant yellow–brown slurry stirred for 5 min. The precipitate was allowed to settle before the supernatant was removed *via* cannula. The complex was then dried *in vacuo* (145 mg, 78.8%) producing a dark, yellow–green solid (found: C, 47.57; H, 4.76; N, 6.01. Calc. for [$C_{35}H_{40}N_4O_6P_2Rh_2$]: C, 47.74; H, 4.58; N, 6.36%). Single crystals suitable for X-ray crystallographic analysis were obtained from a saturated 1 : 1 THF–*n*-pentane solution under Ar atmosphere.

X-Ray structure determinations

(a) General. Data for compounds **5**, **6**, **7**, **9** and **11** were collected using a Bruker SMART 1000 CCD detector/PLATFORM diffractometer[57] using Mo Kα radiation, with the crystals cooled to −80 °C. Data for compound **14** were collected using a Bruker APEX II CCD detector/D8 diffractometer[57] using Mo Kα radiation, with the crystal cooled to −100 °C. The data were corrected for absorption through use of a multi-scan model (SADABS [**5**, **9**, **10**, **11**, **14**] or TWINABS [**6**]) or through Gaussian integration from indexing of the crystal faces (**7**). Structures were solved using the direct methods programs SHELXS–97[58] (**5**, **7**, **9**, **10**, **11**) and SIR97[59] (**14**), or the Patterson search/structure expansion facilities within the DIRDIF-99[60] program system (**6**). Refinements were completed using the program SHELXL-97.[58] Hydrogen atoms were assigned positions based on the sp^2 or sp^3 hybridization geometries of their attached carbon or nitrogen atoms, and were given thermal parameters 20% greater than those of their parent atoms. See Table 2 for a listing of crystallographic experimental data.

(b) Special refinement conditions. (i) Compound **5**: attempts to refine peaks of residual electron density as solvent (DCM) carbon or chlorine atoms were unsuccessful. The data were corrected for disordered electron density through use of the SQUEEZE procedure as implemented in PLATON.[61] A total solvent-accessible void volume of 237.7 $Å^3$ with a total electron count of 83 (consistent with two molecules of solvent dichloromethane, or 0.25 molecules per formula unit of the complex molecule) was found in the unit cell.

(ii) Compound **6**: the crystal used for data collection was found to display non-merohedral twinning. Both components of the twin were indexed with the program CELL_NOW.[62] The second twin component can be related to the first component by 180° rotation about the [−1/4 1 0] axis in real space and about the [0 1 0] axis in reciprocal space. Using all reflection data (exactly overlapped, partially overlapped and non-overlapped), integrated intensities for the reflections from the two components were written into a SHELXL-97 HKLF 5 reflection file with the data integration program SAINT (version 7.06A).[63]

(iii) Compound **10**: the disordered dichloromethane electron density was treated in the same manner as for **5**. A total solvent-accessible void volume of 445.8 $Å^3$ with a total electron count of 125 (consistent with three molecules of solvent dichloromethane, or 0.75 molecules per formula unit of the complex molecule) was found in the unit cell.

Results and discussion

P,*N*-Ligands

The simple, five-step, one-pot syntheses of the targeted (*o*-*N*-methylanilinyl)phosphine compounds, **1–4**, as illustrated in Scheme 1, were carried out using the method reported by Budzelaar for the synthesis of diphenyl(*o*-*N*-methylanilinyl)phosphine[64] (**1**), which was in turn based on the methodology of Katritzky *et al.*[65] Synthetic versatility was achieved using the commercially available phosphorus synthons, chlorodiphenylphosphine (Ph_2PCl), dichlorophenylphosphine ($PhPCl_2$), trichlorophosphine (PCl_3) and bis(dichlorophosphino)methane ($Cl_2PCH_2PCl_2$) in conjunction with the nitrogen-containing precursor, *N*-methylaniline. None of the prepared *P*,*N*-ligands was sensitive to air or water and all were readily soluble in ether, enabling their purification by standard ether extraction. The toxic and odorous byproducts of the hydrolysis of chlorophosphines are typically water-soluble and were removed during the aqueous work-up along with any unreacted lithium reagents. In general, these ligands are thermally stable, white solids and can be purified by recrystallization from a minimal amount of boiling ethanol.

Table 2 Crystallographic experimental details

Compound	**5**·0.25CH_2Cl_2	**6**·0.5CH_2Cl_2	**7**	**9**	**10**·0.75CH_2Cl_2	**11**	**14**·C_4H_8O
Formula	$RhCl_{1.5}PONC_{20.25}H_{18.5}$	$RhCl_2PON_2C_{21.5}H_{22}$	$RhClPON_3C_{22}H_{24}$	$RhClPON_3C_{25}H_{30}$	$Rh_2Cl_{3.5}P_2O_2N_4C_{31.75}H_{35.5}$	$Rh_2Cl_2P_2O_2N_4C_{35}H_{42}$	$Rh_2P_2O_7N_4C_{39}H_{48}$
Formula weight	478.92	529.19	515.77	557.85	896.98	889.39	952.57
Crystal dimens./mm	0.43 × 0.33 × 0.09	0.50 × 0.34 × 0.17	0.43 × 0.41 × 0.26	0.44 × 0.12 × 0.12	0.33 × 0.21 × 0.09	0.38 × 0.38 × 0.16	0.53 × 0.34 × 0.26
Crystal system	Monoclinic	Triclinic	Triclinic	Monoclinic	Monoclinic	Orthorhombic	Monoclinic
Space group	$P2_1/n^a$	$P\bar{1}$ (No. 2)	$P\bar{1}$ (No. 2)	$P2_1/n^a$	$P2_1/n^a$	$P2_12_12_1$ (No. 19)	$P2_1/n^a$
a/Å	10.2776 (8)	12.768 (2)	9.3726 (8)	9.3735 (9)	11.6270 (8)	17.363 (3)	11.2965 (5)
b/Å	34.571 (3)	13.306 (2)	11.3968 (10)	15.9907 (15)	18.1593 (12)	20.180 (3)	25.9075 (11)
c/Å	11.5554 (9)	14.389 (2)	11.4388 (10)	17.1786 (16)	17.4024 (12)	20.910 (3)	14.7517 (6)
α/°		84.988 (2)	85.0063 (12)				
β/°	103.2770 (10)	76.837 (2)	77.9072 (12)	100.0340 (10)	104.6430 (11)		108.5840 (10)
γ/°		74.965 (2)	72.8739 (11)				
V/Å^3	3996.0 (5)	2297.7 (6)	1141.36 (17)	2535.5 (4)	3555.0 (4)	7326.5 (18)	4092.2 (3)
Z	8	4	2	4	4	8	4
ρ_{calcd}/g cm^{-3}	1.592	1.530	1.501	1.461	1.676	1.613	1.546
μ/mm^{-1}	1.144	1.060	0.953	0.864	1.317	1.171	0.937
$2\theta_{max}$/°	52.78	55.18	54.90	52.78	52.80	55.20	55.00
Total data collected	30 586 ($-12 \le h \le 12$, $-43 \le k \le 43$, $-14 \le l \le 14$)	17 407 ($-15 \le h \le 16$, $-17 \le k \le 17$, $0 \le l \le 18$)	10 067 ($-12 \le h \le 12$, $-14 \le k \le 14$, $-14 \le l \le 14$)	18 416 ($-11 \le h \le 11$, $-19 \le k \le 20$, $-21 \le l \le 21$)	25 488 ($-14 \le h \le 14$, $-22 \le k \le 22$, $-21 \le l \le 21$)	62 099 ($-22 \le h \le 22$, $-26 \le k \le 26$, $-26 \le l \le 27$)	35 647 ($-14 \le h \le 14$, $-33 \le k \le 33$, $-19 \le l \le 19$)
Independ. reflns (R_{int})	8169 (0.0275)	17 407 (0.0000)	5172 (0.0119)	5195 (0.0304)	7269 (0.0394)	16 892 (0.0826)	9382 (0.0165)
Obsd reflns [$I \ge 2\sigma(I)$]	7347	12 537	4964	4574	5696	14 226	8686
Restraints/params	0/451	0/519	0/264	0/289	0/388	0/847	0/493
Flack abs. parameter						–0.03(2)	
Goodness-of-fit (all data)	1.137	0.971	1.104	1.052	1.036	1.053	1.050
R_1 [$I \ge 2\sigma(I)$]	0.0307	0.0400	0.0206	0.0247	0.0355	0.0424	0.0227
wR_2 [all data]	0.0746	0.0956	0.0576	0.0696	0.0871	0.0980	0.0598
Largest diff. peak, hole/e Å^{-3}	0.879, –0.449	1.143, –0.800	0.484, –0.589	0.691, –0.317	0.670, –0.603	1.516, –0.778	0.723, –0.365

[a] An alternate setting of $P2_1/c$ (No. 14).

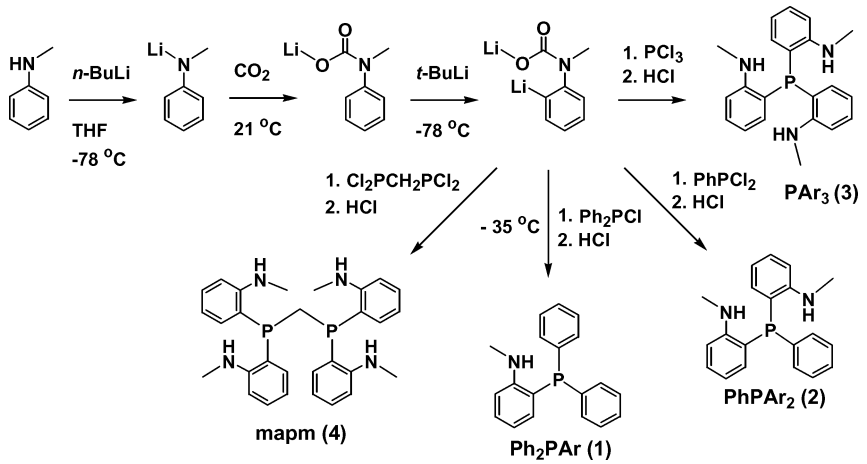

Scheme 1 Ligand syntheses (**1–4**).

We suggest that increased steric congestion at phosphorus after each subsequent *ortho*-arylation of the phosphine tends to hinder production of the more heavily aminated *P*,*N*-ligands as illustrated by the lower yields of these targets.

The challenge of synthesizing (*o*-*N*-methylanilinyl)phosphines can be attributed to the reactivity of the 2° amino group of *N*-alkylanilines[66] that, under basic nucleophilic conditions, leads to unwanted side reactions, thereby necessitating its protection (with CO_2 to afford the *O*-lithiocarbamate) prior to *ortho*-functionalization of the arene. *o*-Metallation to afford the dilithiated intermediate is problematic and rigorous exclusion of air and moisture is required. In this step it is necessary to use the more basic *t*-BuLi as the *o*-metallating agent since *n*-BuLi failed to react with the *O*-lithiocarbamate precursor. For example, in attempts to use *n*-BuLi as the *o*-metallating agent for the preparation of compound **4**, bis(di-*n*-butylphosphino)methane—resulting from reaction of the precursor, bis(dichlorophosphino)methane, with *n*-BuLi that had failed to react in the *o*-metallation step—was instead isolated in quantitative yield.

Very recently, Lee and co-workers have reported that addition of 1 equiv. of THF in diethyl ether significantly enhanced product yields for syntheses involving the *o*-metallation of tetrahydroquinoline[67] derivatives with *t*-BuLi. We have not yet used this methodology to determine the effect of adding stoichiometric THF on product yields of (*o*-*N*-methylanilinyl)phosphines.

^{1}H NMR spectra of the ligands exhibit broad NH signals (due to quadrupolar broadening by nitrogen) between δ_H 4.6 and 4.9 with the general trend that less shielded NH protons belong to the more heavily aminated phosphines. The ^{1}H NMR signals of the NMe protons at *ca.* δ_H 2.8 appear either as broad singlets or as doublets at ambient temperature, the latter situation arising from observable, vicinal coupling to the NH protons ($^3J_{HH}$ = *ca.* 5 Hz). ^{31}P{^{1}H} NMR signals within the series of monophosphines show a significant upfield shift of the singlet resonances (from δ_P −21.8 to −53.6) as the number of amino substituents increases (from one to three), whereas the diphosphine mapm (**4**) exhibit a signal at an even higher field, at δ_P −60.9.

Mononuclear complexes

Mononuclear rhodium complexes were readily prepared by the reaction of the above monophosphine *P*,*N*-ligands (**1–3**) with [Rh(μ-Cl)(COD)]$_2$ at ambient temperature under strictly inert conditions in dichloromethane, before passing carbon monoxide through the reaction mixtures (Scheme 2). The complexes were then precipitated by addition of *n*-pentane and were obtained in moderate to high yields. A more direct route using [Rh(μ-Cl)(CO)$_2$]$_2$ as a starting material had previously been exploited by Roundhill *et al.* to prepare the *N*,*N*-dimethylanilinyl compound, [RhCl(CO)(Ph$_2$PAr′)],[68] and we have also used this methodology to prepare [RhCl(CO)(PAr$_3$)] (**7**). The monophosphines, PhPAr′$_2$ and PAr′$_3$, first prepared by Venanzi and coworkers,[54] have also been used to prepare the *N*,*N*-dimethyl analogues of **6** and **7**, [RhCl(CO)(PhPAr′$_2$)] (**8**) and [RhCl(CO)(PAr′$_3$)] (**9**), respectively. At 27 °C the ^{1}H NMR signal for the NMe protons of [RhCl(CO)(Ph$_2$PAr)] (**5**) appears as a fully resolved doublet with $^3J_{HH}$ = 6.5 Hz. The complexes, [RhCl(CO)(PhPAr$_2$)] (**6**), [RhCl(CO)(PAr$_3$)] (**7**), [RhCl(CO)(PhPAr′$_2$)] (**8**) and [RhCl(CO)(PAr′$_3$)] (**9**), which contain coordinated and pendent amine groups (*vide infra*) all display only a single ^{1}H NMR resonance for *N*-methyl protons at ambient temperature, indicating the rapid exchange of these coordinated and pendent groups—a feature indicative of the (Type II) hemilabile nature of these complexes.[21] Within the series of compounds, **5–9**, the greater the number of anilinyl substituents on the phosphine, the greater the shielding of the ^{31}P nuclei and the greater the $^1J_{RhP}$ (Table 1).

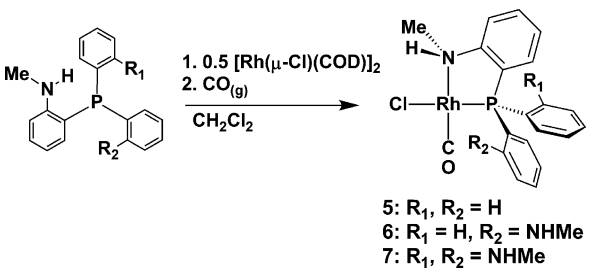

Scheme 2 Syntheses of mononuclear rhodium complexes (**5–7**).

In order to determine how the degree of *N*-methyl substitution affects the lability of the anilinyl groups, we carried out variable temperature NMR experiments on the related dimethyl- and monomethylanilinyl complexes, [RhCl(CO)(PhPAr′$_2$)] (**8**; Ar′ = C$_6$H$_4$NMe$_2$) and [RhCl(CO)(PhPAr$_2$)] (**6**; Ar = C$_6$H$_4$NHMe),

respectively. Upon cooling to –20 °C, ^{1}H NMR analysis of [RhCl(CO)(PhPAr′$_2$)] (**8**) reveals significant broadening of the single resonance representing all *N*-methyl protons, and at –71 °C three distinct signals are evident, in a 1 : 1 : 2 intensity ratio—two for the diastereotopic methyl groups of the coordinated amine, and one for both methyl groups of the pendent amine (Scheme 3)—indicating that amine exchange at rhodium is slow on the NMR timescale at that temperature. Upon further cooling to –79 °C, four distinct *N*-methyl proton resonances of equal intensity are present in the spectrum suggesting that lone-pair inversion of the pendent amine has slowed to allow the resolution of the two chemically unique environments at this nitrogen.

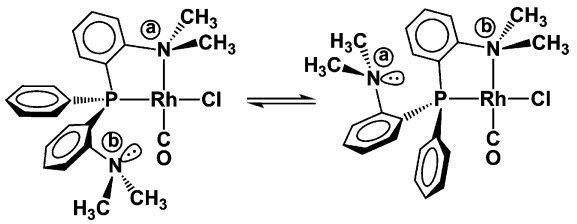

Scheme 3 Enantiomerization of [RhCl(CO)(PhPAr′$_2$)] (**8**).

The variable-temperature ^{1}H NMR spectroscopic study of [RhCl(CO)(PhPAr$_2$)] (**6**) proves to be more complicated than that of its dimethylated counterpart (**8**). As is immediately apparent from Scheme 4, any particular coordination geometry of the complex possesses two stereogenic centers (one at phosphorus, the other at the coordinated amine) giving rise to four stereoisomers existing as two diastereomeric pairs of enantiomers (A/A′ and B/B′). The ^{1}H NMR spectrum of [RhCl(CO)(PhPAr$_2$)] (**6**) at 27 °C reveals two broad, nearly coalescing signals representing two diastereomeric pairs of enantiomers, the intensity ratio of which is approximately 3 : 1, suggesting a thermodynamic preference for one pair of rapidly interconverting enantiomers over the other. The relative concentrations of the diastereomers, which also provide a measure of the equilibrium constant for the diastereoisomerization *via* amine–donor exchange, only vary from 2.80 at 13 °C, to 3.20 at –60 °C. Subsequently, values of *K* for the diastereoisomerization

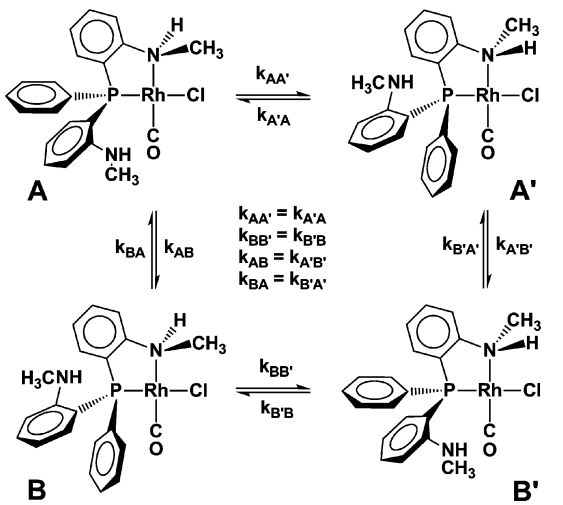

Scheme 4 Possible isomerization mechanisms of [RhCl(CO)(PhPAr$_2$)] (**6**) depicting the possibility of four kinetically independent mechanisms of amine donor exchange at rhodium.

at the temperatures 13, –20 and –60 °C were used to calculate ΔG for this process [eqn (1)], giving a value of 2.3 ± 0.5 kJ mol^{-1} at 95% confidence. We assume that the major diastereoisomeric pair corresponds to the pair of enantiomers B/B′, on the basis of steric considerations, in which the methyl group on the coordinated anilinyl moiety avoids the larger pendent anilinyl substituent in favor of the smaller phenyl group, and on the basis of its having a lower dipole moment which should be favored in the low-polarity solvent. This is also the structure found in the solid state for **6** (*vide infra*).

$$\Delta G_{\text{diaster}} = -RT \ln(K_{\text{diaster}}) \quad (1)$$

Cooling to 13 °C results in the resolution of the two different *N*-methyl signals (for the coordinated and pendent amines) of the major enantiomeric pair into two doublets indicating the coalescence point for this enantiomerization. At 10 °C the *N*-methyl signal for the minor enantiomeric pair begins to split into two more doublets indicating the coalescence point for the enantiomerization of the minor stereoisomers (proposed to result from A ⇌ A′, Scheme 4).

Line-shape analyses for the methyl resonances of [RhCl(CO)(PhPAr$_2$)] (**6**) and [RhCl(CO)(PhPAr′$_2$)] (**8**) were undertaken to compare the rates of exchange processes within these compounds along with the corresponding values of $\Delta G^{\ddagger}$, calculated using eqn (2).[69]

$$k = (k_B T)/h \exp[-\Delta G^{\ddagger}/(RT)] \quad (2)$$

For compound **6**, the rate of enantiomerization for the major stereoisomers (presumably $k_{BB'} = k_{B'B}$) was determined as 17 s^{-1} at 286 K and this value was used to calculate $\Delta G^{\ddagger}$ (286K) = 63.2 kJ mol^{-1}. Similarly, the rate of enantiomerization for the minor stereoisomers (presumably $k_{AA'} = k_{A'A}$) was determined as 25 s^{-1} at 283 K and this value was used to calculate $\Delta G^{\ddagger}$ (283K) = 61.6 kJ mol^{-1}. Exchange parameters for the enantiomerization of the *N*,*N*-dimethyl analogue, **8**, were also obtained: k(194 K) = 274 s^{-1}, $\Delta G^{\ddagger}$ (194K) = 38.4 kJ mol^{-1}. A comparison of the $\Delta G^{\ddagger}$ values for compounds **6** and **8** indicates that, despite its stronger Lewis basicity, the *N*,*N*-dimethylanilinyl group of **8** renders the complex much more labile than its monomethylated counterpart, **6**. This labilization of the dimethylanilinyl donor can be rationalized on the basis of the more severe steric repulsion involving its more highly substituted anilinyl groups (*vide infra*).

The ^{1}H NMR spectrum of [RhCl(CO)(PAr$_3$)] (**7**) at –20 °C displays three well-resolved doublets representing all mutually non-equivalent *N*-methyl groups, while at 27 °C, a rapid three-site exchange process results only in a broad singlet. The ^{1}H NMR spectrum of [RhCl(CO)(PAr′$_3$)] (**9**) exhibits only one signal for all methyl protons at room temperature but, interestingly, at –80 °C only two methyl signals are observed, each integrating as 9 protons. The appearance of two equal-intensity methyl resonances in the low-temperature spectrum of **9** can be rationalized by the geometry of the PAr′$_3$ ligand of **9** in the solid state (*vide infra*), in which the pendent amine groups each have methyl groups in clearly different environments. It appears that rapid exchange of the amine donors at rhodium by rotation about the Rh–P bond, even at –80 °C, occurs in a propeller-like manner, resulting in two chemically distinct average methyl environments in solution.

In order to compare the structural differences between the monomethyl- and dimethylanilinyl analogues, the single-crystal

X-ray structures of the three mononuclear [RhCl(CO)(L)] complexes (L = Ph_2PAr (**5**), $PhPAr_2$ (**6**), PAr_3 (**7**); Ar = *o*-C_6H_4NHMe) have been determined and are compared to the previously reported dimethylanilinyl complex, [RhCl(CO)(Ph_2PAr')] (Ar′ = *o*-$C_6H_4NMe_2$).[70] In addition, we have determined the structure of the compound [RhCl(CO)(PAr'_3)] (**9**) as a further comparison. The ORTEP diagrams of compounds **5**, **6**, **7** and **9** are shown in Fig. 1 and a comparison of their structural parameters, along with those of [RhCl(CO)(Ph_2PAr')], is given in Table 3. All compounds have the expected square-planar geometry at rhodium in which the carbonyl ligand is opposite the weaker *trans*-directing amine group while the chloro ligand is opposite the phosphine moiety which has the greater *trans* effect. All five compounds also have quite comparable structural parameters in which the bond lengths and angles are as expected. Certainly, within the series of monomethylanilinyl complexes (**5–7**) all related parameters are closely comparable, indicating that the incorporation of additional *N*-methylanilinyl groups (Ph_2PAr *vs.* $PhPAr_2$ *vs.* PAr_3) has no obvious structural influence on the metal coordination geometries, although minor differences in the orientations of the aryl groups are observed between the three complexes. Similarly, within the pair of dimethylanilinyl compounds the structural parameters are closely comparable. However, a comparison of the monomethyl- and dimethylanilinyl compounds shows significant differences between the two classes. A visual comparison of the two trisubstituted species **7** and **9**, shown in Fig. 1, indicates that the most significant differences between the monomethyl- and dimethylanilinyl analogues relate to the coordinated amine groups. In the case of the dimethylanilinyl-containing compounds, [RhCl(CO)(Ph_2PAr')] and **9**, the Rh–N distance (2.1947(6) and 2.2019(6) Å, respectively) is greater than that for the three monomethylanilinyl-containing species (av. 2.135(5) Å). This lengthening for the dimethylated compounds is also accompanied by a slight widening of the N–Rh–Cl angle, which is greater than 90° for the dimethylanilinyl compounds and less than 90° for the monomethylanilinyl analogues. Both differences appear to result from the greater steric crowding in the dimethylamines, which weakens the Rh–N bond and gives rise to greater repulsions involving the adjacent chloro ligand. These structural comparisons are consistent with the significantly greater lability of the dimethylanilinyl species as discussed above for compounds **6** and **8**.

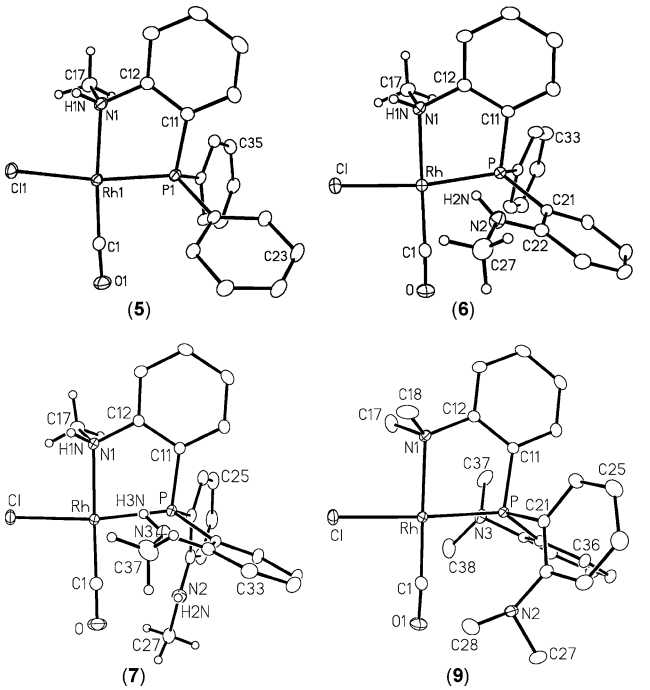

Fig. 1 ORTEP diagrams showing one of two crystallographically independent molecules of [RhCl(CO)(Ph_2PAr)] (**5**), and one of two crystallographically independent molecules of [RhCl(CO)($PhPAr_2$)] (**6**), [RhCl(CO)(PAr_3)] (**7**) and [RhCl(CO)(PAr'_3)] (**9**). Gaussian ellipsoids for all non-hydrogen atoms are depicted at the 20% probability level. Hydrogens are shown artificially small, except for aryl hydrogens which are omitted.

We had initially intended to compare the above monophosphine complexes with the mononuclear diphosphine equivalent, [RhCl(CO)(*P*,*N*-mapm)], for which we had assumed a phosphine binding mode, analogous to compounds **5–9** (in which the diphosphine ligand is bound to Rh *via* one phosphorus and an adjacent amine, while the other end of the diphosphine remains uncoordinated and pendent), would be observed. The related complex, [RhCl(CO)(*P*,*N*-dmapm)], was previously shown to have this structure type.[43] However, all attempts to prepare this mononuclear mapm analogue gave the binuclear diphosphine-bridged species, [$Rh_2Cl_2(CO)_2$(μ-mapm)] (*vide infra*), as the major

Table 3 Selected structural parameters for the mononuclear complexes

	[RhCl(CO)(Ph_2PAr)] (**5**)	[RhCl(CO)($PhPAr_2$)] (**6**)	[RhCl(CO)(PAr_3)] (**7**)	[RhCl(CO)(Ph_2PAr')][70]	[RhCl(CO)(PAr'_3)] (**9**)
Atoms	Bond lengths/Å	Bond lengths/Å	Bond lengths/Å	Bond lengths/Å	Bond lengths/Å
Rh–P	2.1933(7), 2.1909(7)[a]	2.2150(8), 2.2035(8)[a]	2.2199(4)	2.1947(6)[b]	2.2019(6)
Rh–N(1)	2.129(2), 2.140(2)	2.131(2), 2.139(2)	2.1368(13)	2.1865(2)	2.1883(18)
Rh–C(1)	1.819(3), 1.809(3)	1.825(3), 1.819(3)	1.8160(17)	1.807(2)	1.801(3)
Rh–Cl	2.3936(7), 2.3757(7)	2.3786(8), 2.3797(8)	2.3787(4)	2.3867(7)	2.3941(6)
Atoms	Angles/°	Angles/°	Angles/°	Angles/°	Angles/°
P–Rh–N(1)	83.49(6), 83.24(7)	83.28(6), 82.83(7)	84.05(4)	85.03(5)	84.62(5)
Cl–Rh–N(1)	86.69(6), 89.11(7)	88.13(6), 87.16(7)	88.16(4)	91.11(5)	92.17(5)
Cl–Rh–C(1)	98.04(9), 95.36(10)	92.87(9), 96.06(10)	93.16(5)	92.62(7)	90.08(7)
P–Rh–C(1)	91.83(9), 92.65(10)	95.71(9), 94.07(10)	95.00(6)	91.24(7)	93.86(8)

[a] Two crystallographically independent molecules. [b] Correct bond lengths and angles for [RhCl(CO)(Ph_2PAr')] obtained from Table 5 within ref. 70.

product accompanied by minor amounts of uncharacterized side products. None of these side products displayed spectra characteristic of our targeted mononuclear species. It appears that the greater steric accessibility of the mapm ligand favors the formation of the bimetallic complexes over the mononuclear pendent complexes.

Binuclear complexes

The binuclear mapm-bridged complex $[Rh_2Cl_2(CO)_2(\mu\text{-mapm})]$ (**10**; mapm = $Ar_2PCH_2PAr_2$) was prepared, as alluded to above, by adding THF to a flask containing $[Rh(\mu\text{-Cl})(CO)_2]_2$ and mapm (**4**) at ambient temperature; the dmapm analogue, $[Rh_2Cl_2(CO)_2(\mu\text{-dmapm})]$ (**11**; dmapm = $Ar'_2PCH_2PAr'_2$) was prepared by a similar procedure (Scheme 5). Compound **11** had been previously reported[71] but had not been structurally characterized. We were interested in establishing the structural differences that would result from substituting the amine hydrogen in **10** by a methyl group, and also in whether such a substitution would influence the lability of the coordinated amine groups. Both compounds display a single carbonyl stretch in the IR spectrum at around 2000 cm^{-1}, characteristic of Rh(I), and also show a doublet of doublets for the pair of carbonyls in the $^{13}C\{^1H\}$ NMR spectra at around δ_C 186, displaying typical one-bond coupling to Rh and two-bond coupling to P (see Table 1). At ambient temperature the ^1H NMR spectrum of **11** shows a well-resolved broad triplet resonance at δ_H 4.59 ($^2J_{PH}$ = 12.4 Hz) for the methylene group of the dmapm ligand, but shows only very broad, unresolved resonances for the methyl groups, between approximately δ_H 2.2 and 3.7, and for the aromatic protons. Upon cooling to –80 °C the methyl resonances appear as sharp singlets at δ_H 3.68, 2.86, 2.70 and 2.27, each integrating as six protons while the signal for the methylene protons also sharpens significantly.

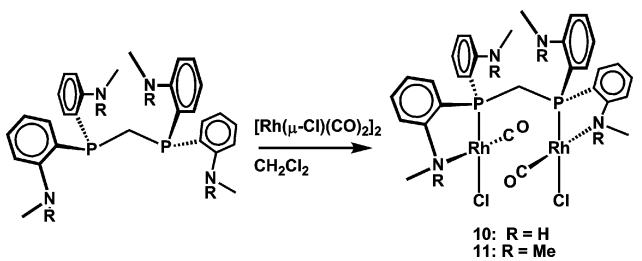

Scheme 5 Preparations of $[Rh_2Cl_2(CO)_2(\mu\text{-mapm})]$ (**10**) and $[Rh_2Cl_2(CO)_2(\mu\text{-dmapm})]$ (**11**).

This temperature dependence suggests fluxionality, presumably involving the sequential exchange of dimethylanilinyl groups at each Rh *via* a transient C_s-symmetric intermediate that renders the methylene hydrogens inequivalent. The ^1H NMR temperature dependence is paralleled by differences in the ^{31}P NMR spectra in which the diphosphine appears as a broad doublet at δ_P 41.0 ($^1J_{RhP}$ = 173 Hz) at ambient temperature but sharpens to a well-resolved multiplet characteristic of an AA′XX′ spin system at –80 °C. In contrast, the resonances in the ^1H and the $^{31}P\{^1H\}$ NMR spectra of the mapm analogue (**10**) are sharp and well resolved, showing no evidence of fluxionality over the full temperature range between 25 °C and –80 °C. In the ^1H NMR spectrum the amine hydrogens overlap two aromatic proton resonances at δ_H 7.75 and 6.94 (as indicated by GCOSY NMR analysis which shows strong correlations to *N*-methyl resonances) while the methylene group of the bridging mapm ligand appears as a multiplet at δ_H 3.94. The *N*-methyl groups appear as two sharp doublets at δ_H 3.17 and 2.78. The downfield NH signal of the (presumably) coordinated amine (δ_H 7.75) exhibits a strong GCOSY correlation to the more upfield NMe signal (δ_H 2.78) while the more upfield NH signal (δ_H 6.94) shows a similar correlation to the more downfield NMe signal (δ_H 3.17) providing a means for the assignment of coordinated and pendent NMe signals. In the $^{31}P\{^1H\}$ NMR spectrum a well-resolved multiplet, resembling the low-temperature resonance for **11**, appears at δ_P 23.3. The observed and simulated[56] $^{31}P\{^1H\}$ NMR spectra, assuming an AA′XX′ spin system, for compounds **10** and **11** are given in Fig. 2. All derived parameters (**10**: $^1J_{RhP}$ = 157 Hz, $^2J_{PP}$ = 53.6 Hz, $^3J_{RhP}$ = 3.2 Hz, $^2J_{RhRh}$ = –0.05 Hz; **11**: $^1J_{RhP}$ = 176 Hz, $^2J_{PP}$ = 46.1 Hz, $^3J_{RhP}$ = 2.7 Hz, $^2J_{RhRh}$ = –0.05 Hz) are consistent with those reported for the related diphosphine-bridged species $[Rh_2(\mu\text{-Cl})(COD)_2(\mu\text{-dppm})][BF_4]$ (dppm = $Ph_2PCH_2PPh_2$).[72] As noted for the monophosphine compounds, substitution of the amine hydrogen in **10** by a methyl group to give **11** substantially labilizes this coordinated amine, again probably due to steric repulsions between this larger tertiary amine and other ligands on Rh. Although exchange between the free and coordinated aniline groups in **11** is facile at ambient temperature, there is no evidence of fluxionality at this temperature for **10**.

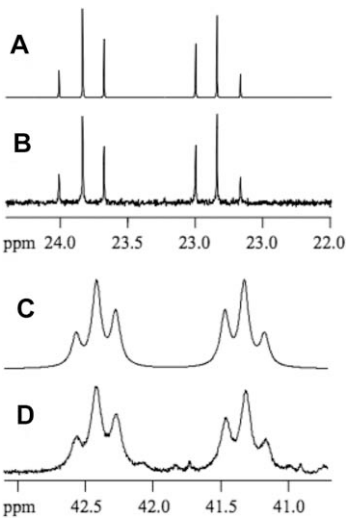

Fig. 2 Calculated (A) and observed (B) $^{31}P\{^1H\}$ NMR spectra of compound **10** at 27 °C. Calculated (C) and observed (D) $^{31}P\{^1H\}$ NMR spectra of compound **11** at –40 °C.

In order to gain a better understanding of the influence of the additional *N*-methyl substituent we have carried out the X-ray structure determination of compounds **10** and **11** and both structures are shown in Fig. 3, with a summary of metrical parameters given in Table 4. Both structures are similar in having a face-to-face arrangement of the two Rh square planes that are bridged by the diphosphine unit of mapm or dmapm and both square planes are also staggered with respect to each other by approximately 40° (**10**) and 44° (**11**), allowing the ligands on one metal to avoid those on the other. Furthermore, in both cases the coordinated aniline group on one metal occupies one side of the approximate Rh_2P_2 plane while that on the other

Table 4 Selected structural parameters for $[Rh_2Cl_2(CO)_2(\mu\text{-mapm})]$ (**10**) and $[Rh_2Cl_2(CO)_2(\mu\text{-dmapm})]$ (**11**)

	$[Rh_2Cl_2(CO)_2(\mu\text{-mapm})]$ (**10**)	$[Rh_2Cl_2(CO)_2(\mu\text{-dmapm})]$ (**11**)
Atoms	Distances/Å	Distances/Å
Rh(1)–Rh(2)	3.4500(4)	4.1211(7), 4.3185(6)[a]
Rh(1)–Cl(1)	2.3810(9)	2.398(1), 2.412(1)
Rh(2)–Cl(2)	2.393(1)	2.396(1), 2.409(1)
Rh(1)–N(1)	2.140(3)	2.181(4), 2.217(4)
Rh(2)–N(3)	2.162(3)	2.200(4), 2.202(4)
Cl(1)–H3N	2.51	
Cl(2)-H1N	2.51	
Atoms	Angles/°	Angles/°
Rh(1)–P(1)–C(3)	116.2(1)	124.8(2), 120.1(2)
Rh(2)–P(2)–C(3)	116.6(1)	122.3(2), 122.8(2)
P(1)–C(3)–P(2)	114.0(2)	118.0(2), 122.0(3)

[a] Two crystallographically independent molecules.

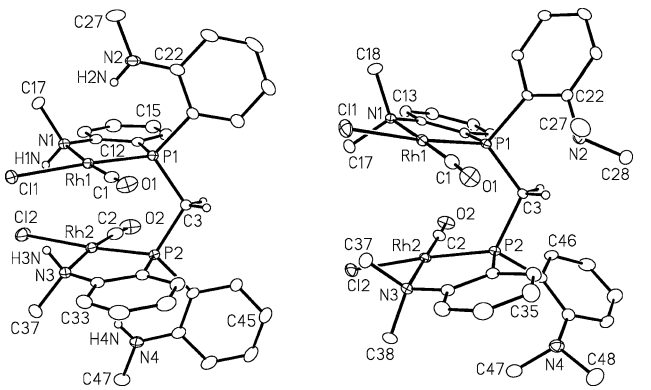

Fig. 3 ORTEP diagrams of $[Rh_2Cl_2(CO)_2(\mu\text{-mapm})]$ (**10**, left) and $[Rh_2Cl_2(CO)_2(\mu\text{-dmapm})]$ (**11**, right). Thermal ellipsoids as in Fig. 1.

metal coordinates to the opposite face such that both complexes are C_2-symmetric. In addition, a slight lengthening of the Rh–Cl bonds is observed in **11** (av. 2.404 Å) compared to **10** (av. 2.387 Å), probably also due to repulsions involving the more bulky dimethylaniline groups. Again, as for the monophosphine analogues discussed above, the Rh–N distances are longer for the dimethylanilinyl complex **11** (2.181(4)–2.217(4) Å) compared to the monomethylanilinyl species **10** (2.140(3), 2.162(3) Å)—a consequence of steric crowding in the former.

However, the major differences between compounds **10** and **11** become obvious on visual comparison of the two in Fig. 3 which demonstrates that the two Rh square planes in **11** are significantly tilted, resulting in a much larger Rh···Rh separation (4.1211(7), 4.3185(6) Å for the two independent molecules) than in **10** (3.4500(4) Å). This tilt of the Rh square planes in **11** is evident in the dihedral angle between these planes of 27.78(5)° and 24.5(1)° in the two independent molecules, whereas the Rh planes in **10** are close to parallel (dihedral angle = 2.93(8)°). The opening up of the cavity between the two Rh square planes in **11** clearly results from repulsion between the chloro ligand on one metal and one methyl of the coordinated dimethylanilinyl group on the adjacent metal, leading to close contacts of *ca.* 2.94 Å between Cl(1) and the methyl hydrogens on C(37), and of *ca.* 2.92 Å between Cl(2) and the C(17) methyl group. Both separations are slightly less than a normal van der Waals separation of 3.00 Å[73] and indicate that these groups are close to their minimum separation. An additional consequence of the above repulsions is the slight bending of the Cl ligands away from these contacts (P(1)–Rh(1)–Cl(1) = 174.51(6)°, 175.79(5)°; P(2)–Rh(2)–Cl(2) = 175.62(5)°, 176.26(5)°). Furthermore, the repulsions that force the Rh planes apart in **11** give rise to significantly enlarged Rh–P–C(3) (av. 122.5 °) and P(1)–C(3)–P(2) (av. 120.0 °) angles compared to those in **10** (116.4 ° and 114.0°, respectively).

In contrast, the contacts between the chloro ligands in **10** and the amino hydrogens (Cl(1)–HN(3) and Cl(2)–HN(1)) associated with the adjacent metal, at 2.51 Å, are much shorter than a normal van der Waals separation[73] and indicate the presence of a reasonably strong hydrogen bond that actually appears to be pulling the metal coordination planes together. This attraction is further manifested in a slight bending of the chlorine ligands *towards* the amine to which it is hydrogen-bonded (P(1)–Rh(1)–Cl(1) = 171.19(4)°; P(2)–Rh(2)–Cl(2) = 171.10(4)°). Interestingly, the pendent methylanilinyl groups in **10** are oriented such that the amino hydrogens are aimed towards the adjacent metals above and below the vacant coordination sites on the outsides of the face-to-face dimer. However, these Rh(1)–HN(2) and Rh(2)–HN(4) contacts (2.59 and 2.57 Å, respectively) appear to be normal and do not suggest an attractive interaction between these hydrogens and the metals. As a consequence, the Rh(1)–P(1)–C(21) and Rh(2)–P(2)–C(41) angles (123.8(1)° and 122.8(1)°) are much larger than the other angles at phosphorus which range from 102.8(1)° to 105.8(2)°, suggesting that the above Rh–H contacts are repulsive, forcing the anilinyl groups away from the metals slightly. Certainly, the downfield shift in the ^{1}H NMR spectrum of these amine hydrogens (δ_H 6.94) argues against an agostic interaction in solution, for which we would expect an upfield shift. Nevertheless, the Rh–H contacts observed in the solid state cannot be too unfavorable, given the orientation of the pendent methylanilinyl groups which project the amine hydrogens into the vicinities of the two metals, rather than away from them as observed for the dimethylanilinyl groups in **11**.

The apparent lack of amine lability in complex **10** prompted our attempts to prepare a species with inherently lower coordinative saturation at the bimetallic core. Specifically, a cationic, chloro-bridged complex similar to $[Rh_2(COD)_2(\mu\text{-Cl})(\mu\text{-dppm})][BF_4]$[72] was targeted in which the remaining chloride was bridging and could serve as a source of coordinative unsaturation. The targeted complex, $[Rh_2(\mu\text{-Cl})(CO)_2(\mu\text{-mapm})]^+$, involving mapm as the bridging diphosphine, was selected due to the proximity of the Rh centers of the parent complex **10** relative to the dmapm analogue, **11**. Unfortunately, reaction of **10** with a variety of silver salts, including $AgBF_4$, $AgPF_6$ and AgOTf, failed to yield the monochloride. Reactions of **10** with $AgBF_4$ and $AgPF_6$ under a variety of conditions and solvent systems routinely resulted in multiple decomposition products, while reaction of **10** with AgOTf yielded the symmetric disubstituted species, $[Rh_2(OTf)_2(CO)_2(\mu\text{-mapm})]$ (**12**) (Scheme 6). The molar conductivity of **12** in CH_3NO_2 was determined to be 23 cm^2 Ω^{-1} mol^{-1}, suggesting some degree of triflate dissociation. Additionally, $^{19}F\{^1H\}$ NMR spectroscopy of **12** at 27 °C reveals two broad coalescing signals suggesting two chemically distinct fluorine environments by a possible exchange of inner- and outer-sphere triflate moieties. $^{31}P\{^1H\}$ NMR spectroscopy of **12** shows a downfield shift (relative to the parent complex, **10**) of the multiplet resonance (δ_P 31.5, $^1J_{RhP}$ = 176 Hz)

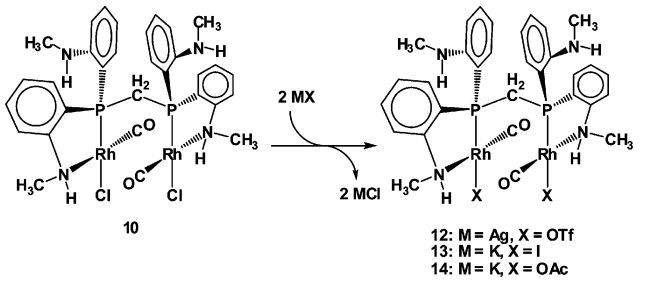

Scheme 6 Chloride-replacement reactions of $[Rh_2Cl_2(CO)_2(\mu\text{-mapm})]$ (**10**).

and the ^{1}H NMR spectrum of **12** is similar to that of **10**. In spite of some degree of apparent triflate ion dissociation, we were unable to isolate the presumed cationic monotriflate species. Expecting that exchange of the chloro substituents of **10** for the larger iodide ions could favor formation of an iodide-bridged species, we synthesized $[Rh_2I_2(CO)_2(\mu\text{-mapm})]$ (**13**, Scheme 6) through reaction of **10** with a five-fold excess of KI in dichloromethane–methanol. However, subsequent reactions of **13** with $AgBF_4$, $AgPF_6$ and AgOTf yielded either decomposition in the first two cases or the bis-triflato species **12**, as was observed for **10**. Although the targeted, cationic, halogeno-bridged complexes could not be prepared, the weakly coordinating sulfonate ligands of **12** appear to be labile, as suggested by the molar conductivity and the observation of both free and coordinated triflate ions in solution. The $^{31}P\{^1H\}$ NMR spectrum of **13**, although similar to **10**, shows a slight upfield shift of the multiplet resonance to δ_P 20.3 with $^1J_{RhP} = 162$ Hz. As expected, the ambient temperature ^{1}H NMR spectrum of **13** is very similar to that of **10**. Unfortunately, $^{13}C\{^1H\}$ spectra for complexes **12** and **13** could not be obtained due to their poor solubilities in a variety of solvents.

The acetato complex, $[Rh_2(OAc)_2(CO)_2(\mu\text{-mapm})]$ (**14**), could also be prepared by reaction of **10** with KOAc in THF. The low molar conductivity of **14** (12 cm^2 Ω^{-1} mol^{-1} in CH_3NO_2) suggests little acetate-ion dissociation, and may result from minor amounts of salt impurities. Interestingly, compound **14** exhibits strong solvatochromic tendencies, transforming from a deep-red solution to a dark, yellow–green powdery solid upon removal of solvent *in vacuo*. Furthermore, the ^{1}H NMR spectrum of this complex exhibits highly deshielded NH protons at δ_H 8.91 and 8.12 which were identified, *via* GCOSY analysis, by their strong correlations to NMe protons. $^{31}P\{^1H\}$ NMR data show the expected multiplet at δ_P 28.2 with $^1J_{RhP} = 155$ Hz. $^{13}C\{^1H\}$ NMR data could not be obtained from CD_2Cl_2 due to decomposition to multiple products in solution over a 24 h period. Interestingly, one of these multiple decomposition products has been identified as $[Rh_2Cl_2(CO)_2(\mu\text{-mapm})]$ *via* ^{31}P NMR spectroscopy. It was also noticed that **14** is quite hygroscopic as a solid, as the incorporation of water, which can be evidenced by ^{1}H NMR, led to its slow decomposition to multiple uncharacterized products, as indicated by ^{31}P NMR.

The structure of **14** has been determined crystallographically, and an ORTEP diagram of this species is shown in Fig. 4. As is obvious from a comparison of Fig. 3 and 4, compounds **10** and **14** have closely related structures. Again, the hydrogen atoms of the coordinated amine are hydrogen bonded to the anionic ligand (in this case acetate) on the adjacent metal, as demonstrated by the close O–H contacts (O(4)–H(3N) = 1.94 Å; O(6)–H(1N) = 1.84 Å). In spite of the larger acetate compared to chloro ligand, the Rh(1)–Rh(2) separation in **14** (3.2227(2) Å) is actually less than in **10** (3.4500(4) Å).

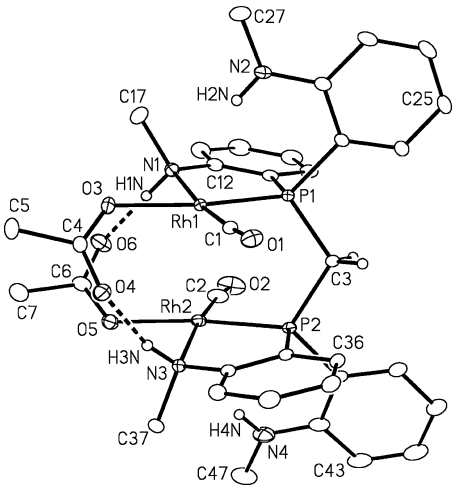

Fig. 4 ORTEP diagram of $[Rh_2(OAc)_2(CO)_2(\mu\text{-mapm})]$ (**14**). Thermal ellipsoids as in Fig. 1.

This mutual approach of both metals results in a slight pyramidalization of both square planes, as shown in Fig. 4, with the metals being 0.08 Å and 0.07 Å out of the planes defined by the four attached ligands. This distortion appears not to result from any mutual attraction of the metals, but instead from repulsion due to pendent amine hydrogens above and below the pair of almost-parallel square planes. We had noted for compound **10** that these contacts (~2.58 Å) were probably repulsive; in **14** the Rh–HN contacts (~2.50 Å) are even shorter and in this case lead to a significant deviation of the metals from their respective planes. Again, the very low-field chemical shifts of these protons (δ_H 8.91, 8.12) argue against any type of agostic interaction in solution, for which we would expect a significant upfield shift.

Conclusions

A number of *P*,*N*-ligated, mono- and binuclear complexes of rhodium have been synthesized and fully characterized. The complexes $[RhCl(CO)(PhPAr_2)]$ (**6**), $[RhCl(CO)(PAr_3)]$ (**7**), $[RhCl(CO)(PhPAr'_2)]$ (**8**), $[RhCl(CO)(PAr'_3)]$ (**9**) and $[Rh_2Cl_2(CO)_2(\mu\text{-dmapm})]$ (**11**) are shown by NMR to display fluxional behavior consistent with the hemilabile nature of these systems. The more highly substituted dimethylanilinyl ligands are found to be more labile than the monomethyl analogues. X-Ray structural comparisons of related dimethyl- and monomethylanilinyl species show greater steric repulsions and concomitant weaker Rh–amine interactions for the former, offering a rationalization for the greater lability of the NMe_2-substituted ligands. The *N*-methylamino-tethered, binuclear complex, $[Rh_2Cl_2(CO)_2(\mu\text{-mapm})]$ (**10**), has a greatly reduced interatomic Rh···Rh separation compared to its *N*,*N*-dimethylated counterpart, $[Rh_2Cl_2(CO)_2(\mu\text{-dmapm})]$ (**11**), owing to greater steric repulsions between the two Rh coordination planes in the latter case. While the mapm-bridged binuclear complex is expected to have greater potential for bimetallic cooperativity owing to significantly closer approach of the metals, it may be that the

lower steric bulk of the monomethylanilinyl group, which allows this closer approach, may actually work to the detriment of the system, owing to the lower lability of these groups. What effects the two competing influences will have must await subsequent reactivity studies.

Our failure to prepare cationic, halide-bridged species probably results from the strain inherent in such a product, in which the halide bridge would be required to lie opposite both ends of the bridging diphosphine. In addition, the staggered arrangement of the Rh coordination planes in the dichloro precursor (**10**) appears necessary in order to minimize unfavorable contacts between these planes. Replacement of one chloride ligand by a bridging arrangement of the remaining chloride would force an eclipsed conformation of the planes leading to a closer and less favorable approach of the anilinyl and carbonyl groups on adjacent metals. Nevertheless, it should still be possible to achieve an anion-bridged structure through the use of bidentate groups such as acetates, which should give rise to less strain while maintaining more favorable contacts between the planes, although we have until now failed to isolate such species in this chemistry.

The subsequent chemistries of the mapm-bridged species **10** and **12–14** will be investigated in order to determine whether ligand hemilability and effects of metal–metal cooperativity will play a role. Furthermore, the potential of using the acetate moieties in **14** as an internal base for deprotonation of one or more of the amine groups to generate catalytically active amido-rhodium species[51] is an immediate goal of these studies.

Acknowledgements

We thank the Natural Sciences and Engineering Research Council of Canada (NSERC) and the University of Alberta for financial support for this research and NSERC for funding the Bruker PLATFORM/SMART 1000 CCD diffractometer, the Bruker D8/APEX II CCD diffractometer and the Nicolet Avatar IR spectrometer. We thank the Department's Analytical and Instrumentation Laboratory for performing elemental analyses as well as the NMR Spectroscopy Laboratory and Mr Rahul Samant for assistance with variable temperature NMR spectroscopic analyses and helpful discussions. We thank Dr Guy Bernard for carrying out ^{31}P NMR spectral simulations.

References

1 A. M. Sargeson, *Pure Appl. Chem.*, 1984, **56**, 1603–1619.
2 S. J. Archibald, *Annu. Rep. Prog. Chem., Sect. A*, 2007, **103**, 264–286.
3 F. T. Edelmann, *Angew. Chem., Int. Ed.*, 2001, **40**, 1656–1660.
4 M. Albrecht and G. van Koten, *Angew. Chem., Int. Ed.*, 2001, **40**, 3750–3781.
5 M. M. Taqui Khan and A. E. Martell, *Inorg. Chem.*, 1974, **13**, 2961–2966.
6 C. A. Bessel, P. Aggarwal, A. C. Marschilok and K. J. Takeuchi, *Chem. Rev.*, 2001, **101**, 1031–1066.
7 J.-C. Hierso, R. Smaliy, R. Amardeil and P. Meunier, *Chem. Soc. Rev.*, 2007, **36**, 1754–1769.
8 J. E. Huheey, E. A. Keiter and R. L. Keiter, *Inorganic Chemistry: Principles of Structure and Reactivity*, HarperCollins, New York, 4th edn, 1993, pp. 522–524.
9 R. J. Puddephatt, *Chem. Soc. Rev.*, 1983, **12**, 99–127.
10 B. Chaudret, B. Delavaux and R. Poilblanc, *Coord. Chem. Rev.*, 1988, **86**, 191–243.
11 A. L. Balch, L. A. Fossett, R. R. Guimerans and M. M. Olmstead, *Organometallics*, 1985, **4**, 781–788.
12 J. Andrieu, P. Braunstein, A. Tiripicchio and F. Ugozzoli, *Inorg. Chem.*, 1996, **35**, 5975–5985.
13 T. K. Ronson, H. Adams and M. D. Ward, *Inorg. Chim. Acta*, 2005, **358**, 1943–1954.
14 M. A. Jalil, S. Fujinami, T. Honjo and H. Nishikawa, *Polyhedron*, 2001, **20**, 1071–1078.
15 K. Mashima, Y. Kaneda, A. Fukumoto, M. Tanaka, K. Tani, H. Nakano and A. Nakamura, *Inorg. Chim. Acta*, 1998, **270**, 459–466.
16 M. E. Broussard, B. Juma, S. G. Train, W.-J. Peng, S. A. Laneman and G. G. Stanley, *Science*, 1993, **260**, 1784–1788.
17 J. P. Farr, M. M. Olmstead, C. H. Hunt and A. L. Balch, *Inorg. Chem.*, 1981, **20**, 1182–1187.
18 F. E. Wood, J. Hvoslef, H. Hope and A. L. Balch, *Inorg. Chem.*, 1984, **23**, 4309–4315.
19 J. C. Jeffrey and T. B. Rauchfuss, *Inorg. Chem.*, 1979, **18**, 2658–2666.
20 C. S. Slone, D. A. Weinberger and C. A. Mirkin, *Prog. Inorg. Chem.*, 1999, **48**, 233–350.
21 P. Braunstein and F. Naud, *Angew. Chem., Int. Ed.*, 2001, **40**, 680–699.
22 P. Espinet and K. Soulantica, *Coord. Chem. Rev.*, 1999, **193–195**, 499–556.
23 P. Braunstein, *J. Organomet. Chem.*, 2004, **689**, 3953–3967.
24 J. Andrieu, J.-M. Camus, P. Richard, R. Poli, L. Gonsalvi, F. Vizza and M. Peruzzini, *Eur. J. Inorg. Chem.*, 2006, 51–61.
25 A. Bader and E. Lindner, *Coord. Chem. Rev.*, 1991, **108**, 27–110.
26 H. Yang, M. Alvarez-Gressier, N. Lugan and R. Mathieu, *Organometallics*, 1997, **16**, 1401–1409.
27 F. Speiser, P. Braunstein and L. Saussine, *Organometallics*, 2004, **23**, 2625–2632.
28 M. Bassetti, *Eur. J. Inorg. Chem.*, 2006, 4473–4482.
29 H. Yang, N. Lugan and R. Mathieu, *Organometallics*, 1997, **16**, 2089–2095.
30 R. Fernández-Galán, F. A. Jalón, B. R. Manzano and J. Rodríguez-de la Fuente, *Organometallics*, 1997, **16**, 3758–3768.
31 M. P. Anderson, A. L. Casalnuovo, B. J. Johnson, B. M. Mattson, A. M. Mueting and L. H. Pignolet, *Inorg. Chem.*, 1988, **27**, 1649–1658.
32 J. C. Jeffrey, T. B. Rauchfuss and P. A. Tucker, *Inorg. Chem.*, 1980, **19**, 3306–3315.
33 I. Bertini, P. Dapporto, G. Fallani and L. Sacconi, *Inorg. Chem.*, 1971, **10**, 1703–1707.
34 A. Del Zotto, G. Nardin and P. Rigo, *J. Chem. Soc., Dalton Trans.*, 1995, 3343–3351.
35 K. V. Baker, J. M. Brown, N. A. Cooley, G. D. Hughes and R. J. Taylor, *J. Organomet. Chem.*, 1989, **370**, 397–406.
36 K. Tani, M. Yabuta, S. Nakamura and T. Yamagata, *J. Chem. Soc., Dalton Trans.*, 1993, 2781–2789.
37 M. Habib, H. Trujillo, C. A. Alexander and B. N. Storhoff, *Inorg. Chem.*, 1985, **24**, 2344–2349.
38 J. P. Farr, F. E. Wood and A. L. Balch, *Inorg. Chem.*, 1983, **22**, 3387–3393.
39 B. R. Aluri, M. K. Kindermann, P. G. Jones, I. Dix and J. Heinicke, *Inorg. Chem.*, 2008, **47**, 6900–6912.
40 M. T. Whited, E. Rivard and J. C. Peters, *Chem. Commun.*, 2006, 1613–1615.
41 M. D. Fryzuk and P. A. MacNeil, *J. Am. Chem. Soc.*, 1981, **103**, 3592–3593.
42 D. Soulivong, C. Wieser, M. Marcellin, D. Matt, A. Harriman and L. Toupet, *J. Chem. Soc., Dalton Trans.*, 1997, 2257–2262.
43 J. N. L. Dennett, M. Bierenstiel, M. J. Ferguson, R. McDonald and M. Cowie, *Inorg. Chem.*, 2006, **45**, 3705–3717.
44 N. D. Jones, P. Meessen, M. B. Smith, U. Losehand, S. J. Rettig, B. O. Patrick and B. R. James, *Can. J. Chem.*, 2002, **80**, 1600–1606.
45 N. D. Jones and B. R. James, *Adv. Synth. Catal.*, 2002, **344**, 1126–1134.
46 S. J. L. Foo, N. D. Jones, B. O. Patrick and B. R. James, *Chem. Commun.*, 2003, 988–989.
47 N. D. Jones, S. J. L. Foo, B. O. Patrick and B. R. James, *Inorg. Chem.*, 2004, **43**, 4056–4063.
48 N. D. Jones, P. Meessen, U. Losehand, B. O. Patrick and B. R. James, *Inorg. Chem.*, 2005, **44**, 3290–3298.
49 S. E. Clapham, A. Hadzovic and R. H. Morris, *Coord. Chem. Rev.*, 2004, **248**, 2201–2237.
50 R. Noyori, *Angew. Chem., Int. Ed.*, 2002, **41**, 2008–2022.
51 P. Maire, T. Büttner, F. Breher, P. Le Floch and H. Grützmacher, *Angew. Chem., Int. Ed.*, 2005, **44**, 6318–6323.

52 G. Giordano and R. H. Crabtree, *Inorg. Synth.*, 1979, **19**, 218–220.
53 J. A. McCleverty, G. Wilkinson, L. G. Lipson, M. L. Maddox and H. D. Kaesz, *Inorg. Synth.*, 1990, **28**, 84–86.
54 H. P. Fritz, I. R. Gordon, K. E. Schwarzhans and L. M. Venanzi, *J. Chem. Soc.*, 1965, 5210–5216.
55 H. Gilman and I. Banner, *J. Am. Chem. Soc.*, 1940, **62**, 344–345.
56 Spectral simulations were carried out using *SpinWorks v. 2.5.5*: K. Marat, SpinWorks, University of Manitoba, Winnipeg, MB, Canada, 2006.
57 Programs for diffractometer operation, unit cell indexing, data collection, data reduction and absorption correction were those supplied by Bruker.
58 G. M. Sheldrick, *Acta Crystallogr., Sect. A*, 2008, **64**, 112–122.
59 A. Altomare, M. C. Burla, M. Camalli, G. L. Cascarano, C. Giacovazzo, A. Guagliardi, A. G. G. Moliterni, G. Polidori and R. Spagna, *J. Appl. Crystallogr.*, 1999, **32**, 115–119.
60 P. T. Beurskens, G. Beurskens, R. de Gelder, S. Garcia-Granda, R. O. Gould, R. Israel and Jan M. M. Smits, *The DIRDIF-99 program system*, Crystallography Laboratory, University of Nijmegen, The Netherlands, 1998.
61 P. van der Sluis and A. L. Spek, *Acta Crystallogr., Sect. A*, 1990, **46**, 194–201; A. L. Spek, PLATON—a multipurpose crystallographic tool, *Acta Crystallogr., Sect. A*, 1990, **46**, C34.
62 G. M. Sheldrick, *CELL_NOW version 2008/2*, University of Göttingen, Germany, 2008.
63 G. M. Sheldrick, *SAINT version 7.06A*, Bruker AXS Inc., Madison, WI, USA, 2003.
64 A. B. van Oort, P. H. M. Budzelaar, J. H. G. Frijns and A. G. Orpen, *J. Organomet. Chem.*, 1990, **396**, 33–47.
65 A. R. Katritzky, W.-Q. Fan and K. Akutagawa, *Tetrahedron*, 1986, **42**, 4027–4034.
66 C. J. Wu, S. H. Lee, S. T. Yu, S. J. Na, H. Yun and B. Y. Lee, *Organometallics*, 2008, **27**, 3907–3917.
67 C. J. Wu, S. H. Lee, H. Yun and B. Y. Lee, *Organometallics*, 2007, **26**, 6685–6687.
68 T. B. Rauchfuss and D. M. Roundhill, *J. Am. Chem. Soc.*, 1974, **96**, 3098–3105.
69 A. D. Bain, *Prog. Nucl. Magn. Reson. Spectrosc.*, 2003, **43**, 63–103.
70 P. Suomalainen, S. Jääskeläinen, M. Haukka, R. H. Laitinen, J. Pursiainen and T. A. Pakkanen, *Eur. J. Inorg. Chem.*, 2000, 2607–2613.
71 N. D. Jones, PhD thesis, University of British Columbia, 2001.
72 F. Lorenzini, K. T. Hindle, S. J. Craythorne, A. R. Crozier, F. Marchetti, C. J. Martin, P. C. Marr and A. C. Marr, *Organometallics*, 2006, **25**, 3912–3919.
73 Y. V. Zefirov and P. M. Zorkii, *Russ. Chem. Rev. (Engl. Transl.)*, 1989, **58**, 421–440.